



Removal of thorium(IV) from aqueous solutions by carboxyl-rich hydrothermal carbon spheres through low-temperature heat treatment in air

Zhi-wei Zhou^{a,b}, Guo-xuan Xiong^{a,b}, Yun-hai Liu^{a,b}, Xiao-hong Cao^{a,b},
Zhi-bin Zhang^{a,b,c,*}

^aState Key Laboratory Breeding Base of Nuclear Resources and Environment (East China Institute of Technology), Ministry of Education, Nanchang 330013, P.R. China, Tel. +86 794 8258320; Fax: +86 8258320; email: zhibzhang@163.com

^bKey Laboratory of Radioactive Geology and Exploration Technology Fundamental Science for National Defense, East China Institute of Technology, Fuzhou 344000, P.R. China

^cEngineering Research Center of Nano-Geomaterials of Ministry of Education, China University of Geosciences, Wuhan 430074, P.R. China

Received 2 September 2013; Accepted 23 February 2014

ABSTRACT

The number of carboxyl groups on the surface of hydrothermal carbon spheres (HCSs) has been largely increased by simply heating at lower temperature in air. The textural properties of the carboxyl-rich hydrothermal carbon spheres were characterized using Boehm titrations, scanning electron microscopy, Fourier transform infrared spectrometer (FT-IR), and elemental analysis (EA). The result of Boehm titrations indicated that the content of carboxyl groups on HCSs increased significantly from 0.53 to 3.81 mmol/g after heat treatment at 300°C, which was also confirmed by FT-IR and EA qualitatively. The ability of heat-treated HCSs has been explored for the removal and recovery of thorium from aqueous solutions, and the influences of different experimental parameters, such as solution pH, heat treatment temperature, contact time, initial thorium concentration, temperature, and ionic strength on adsorption, were investigated. The Th(IV) sorption capacity of HCSs increased from 17.76 to 69.93 mg/g after heat treatment at 300°C for 5 h. Adsorption kinetics was better described by the pseudo-second-order model and the adsorption process was well defined by the Langmuir isotherm. Thermodynamic parameters indicated that the adsorption process was feasible, endothermic, and spontaneous in nature. Selective adsorption studies showed that the heat-treated HCSs could selectively remove Th(IV), and the selectivity coefficients were improved after heat treatment in the presence of coexisting ions, Na(I), Ni(II), Sr(II), Mn(II), Mg(II), Zn(II), and Hg(II). The adsorbed heat-treated HCSs could be effectively regenerated by 1.0 mol/L HCl solution for the removal and recovery of Th(IV). Complete removal (≈100%) of Th(IV) from 1.0 L artificial sea water containing 25.0 mg Th(IV) ions was possible with 1.5 g heat-treated HCSs.

Keywords: Hydrothermal carbon spheres; Adsorption; Carboxyl groups; Thorium

*Corresponding author.

1. Introduction

Thorium is found in the tetravalent state and concentrated in natural sediments either in detrital restate minerals, such as monazite, rutile, and thorianite, or adsorbed onto natural colloidal-sized materials in the nature [1] and has been extensively used in many areas like nuclear fuel, alloy, and laboratory investigations [2]. Besides its industrial importance, these activities generate a wide diversity of wastewaters containing isotopes of thorium and its daughter products, which can cause dangerous consequences for human beings by affecting the ecosystems [3]. The lethal dose of Th^{4+} nitrate or chloride by intravenous injection is 25–30 mg kg^{-1} in rabbits [4]. Therefore, the removal and recovery of thorium from contaminated groundwater has attracted more and more attention.

Over the last few decades, a variety of technologies, such as solvent extraction [5,6], ion exchange [7], and adsorption, have been developed for the removal and recovery of thorium from radioactive wastes in consideration of the dual significance of the potential environmental health threat and use as nonrenewable resource of nuclear energy, among which adsorption is an attractive method because of its high efficiency, ease of handling, and the availability of different adsorbents. Numerous adsorbents have been used for the removal of thorium from the wastewaters, such as natural [8–11] and modified clays [12–17], microorganisms [18], carbon materials [19–21], zeolite [22,23], and cellulosic materials [24].

A promising adsorbent suitable for use in extreme environments, such as high temperature, high radiation damage rate, and aggressive chemical environments, might be carbonaceous materials, because of their higher radiation and thermal and chemical stability than that of organic exchanger resins and familiar inorganic sorbents [24]. Nowadays, carbonaceous materials such as activated carbon [24,25], carbon nanotubes [26,27], carbon fiber [28], and mesoporous carbon [29,30] are being widely used in the area of metal separation and wastewater treatment, but their performances of adsorption are not desirable; furthermore, they are usually prepared under harsh and/or high energy-consuming conditions [31]. Hydrothermal carbon spheres (HCSs) were chosen to be the sorbent in this work. They could be prepared from saccharides and other biomass, such as glucose [32], sucrose [33,34], fructose [35], starch [36], and cellulose [37,38] under facile and mild hydrothermal process without using any organic solvents, catalysts, or surfactants at moderate temperatures [39]. HCSs have the inherent characteristics of carbon materials, such as thermal and radiation stabilities. Meanwhile, HCSs have relatively abundant

oxygen-containing functional groups (OFGs) [40], which make them more advantageous to subsequent surface chemical function and sorption separation.

In our previous work, our group has prepared carboxyl-rich hydrothermal carbon spheres through low-temperature heat treatment in air and found that it is an excellent adsorbent toward uranium (VI) in the aqueous solution, the U(VI) sorption capacity of HCSs increased from 55.0 to 179.95 mg/g after heat treatment at 300 °C for 5 h [41]. However, to the best of our knowledge, the HCSs have not been reported for adsorption of thorium from aqueous system so far. Therefore, it would be interesting to explore the possibility of HCSs for the environmental purpose mentioned above.

In the present report, the carboxyl-rich hydrothermal carbon spheres have been prepared by simply heating at lower temperature in air. Various techniques were used to characterize the structure and textural property of HCSs, including Boehm titrations, Fourier transform infrared spectroscopy (FT-IR), scanning electron microscopy (SEM), and elemental analysis (EA). The ability of heat-treated HCSs has been explored for the removal and recovery of thorium from aqueous solutions. The parameters that affect the thorium(IV) sorption, such as solution pH, contact time, initial thorium(IV) concentration, ionic strength, and temperature, have been investigated. The adsorption achieved equilibrium within 80 min and followed a pseudo-second-order equation. Results have been analyzed by Langmuir and Freundlich isotherm; the former was more suitable to describe the sorption process. Thermodynamic parameters indicated the adsorption process was an endothermic process and spontaneous.

2. Materials and methods

2.1. Materials

For the preparation of a stock thorium(IV) solution, 0.2457 g $\text{Th}(\text{NO}_3)_4 \cdot 5\text{H}_2\text{O}$ was dissolved in 20 mL 0.1 M HCl, and then the solution was transferred to a 100-mL volumetric flask and diluted to the mark with distilled water to produce a thorium(IV) stock solution (1 mg/mL). The thorium solutions were prepared by diluting the stock solution to appropriate volumes depending upon the experimental requirements. All other reagents were of AR grade.

2.2. Preparation of carboxylate-rich hydrothermal carbon spheres

Hydrothermal carbon spheres were prepared according to Wang et al. [32] with minor revision. Typically, 2.0 g glucose and 15 mL deionized water

were transferred into a 25-mL Teflon-lined stainless steel autoclave, sealed, and heated at 180°C for 16 h. When the reaction was completed, the autoclave was cooled to room temperature, and the black precipitate was collected and washed with water, pure ethanol, and acetone until the filtrate was neutral, and the final product was dried at 80°C for 6 h and was designated as HCSs.

The HCSs were then further treated in a muffle furnace in air at a temperature range of approximately 100–300°C. The heat-treated solids were washed thoroughly with deionized water and subsequently ethanol until neutral and then dried in a vacuum oven at 50°C for 12 h. The heat-treated samples were denoted as HCSs-100, if heat-treated at 100°C, and so on.

2.3. Characterization

The OFGs content of HCSs was examined by Boehm titrations [42]. Surface morphology was characterized on a JEOL JSM-5900 scanning electron microscopy. The FT-IR spectra were recorded on Nicolet Nexus 870 Fourier transform infrared spectrometer using the KBr pellet technique (1:50) with the resolution 2 cm⁻¹. CHN content was determined by a CARLO1106 elemental analysis device.

2.4. Adsorption experiments

The Th(IV) adsorption was studied as a function of pH, heat treatment temperature, contact time, initial thorium concentration, temperature, and ionic strength. The batch sorption studies were performed in a reciprocating water bath shaker with concussion speed of 200 rpm. In the experiments, 50 mg of sorbent was suspended in 50 mL solution containing different amounts of Th(IV) concentration and different initial pH (adjusted with 0.1 mol/L HCl and 0.1 mol/L NaOH). The concentration of thorium ions in the solution was determined by the arsenazo III method with a 721-type spectrophotometer at 665 nm [10]. The amount of thorium ions adsorbed per unit mass of the HCSs and the Th(IV) removal were calculated by Eqs. (1) and (2).

$$q_e = \frac{(C_i - C_e)V}{W} \quad (1)$$

$$\text{Removal}/\% = \frac{C_0 - C_e}{C_0} \cdot 100\% \quad (2)$$

where q_e is the adsorption capacity of the HCSs (mg/g); C_0 and C_e are the thorium concentration in the initial and equilibrium solution (mg/L), respectively; C_i is the

thorium concentration of the initial solution subtracted the precipitated part at the fixed pH; V is the volume of aqueous solution (L); and W is the mass of HCSs (g).

3. Results and discussion

3.1. Characterization

The weight-loss ratios, elemental analyses, and carboxyl content of the heat-treated HCSs are shown in Table 1. Notably, the weight-loss ratio became higher with the increase in temperature, probably due to the volatilization and decomposition of some incompletely polymerized monomers, oligomers, and/or small molecules on HCSs frameworks. The content of carboxyl groups increased from 0.53 to 3.60 mmol/g after heating at 300°C for 1 h, and only to 3.81 mmol/g for 5 h. It could be deduced that the formation of freshly generated carboxyl groups was a relatively rapid chemical process and the heating time had little influence on the carboxyl group content. It was shown that there was no nitrogen in any tested samples, so the oxygen content can be calculated by subtracting the sum of carbon and hydrogen from 100. Both $C\%$ and $H\%$ decreased remarkably with the heat treatment temperature increasing, which also supported the results from Boehm titration and FT-IR spectra below.

The FT-IR spectra of the pristine and heat-treated HCSs are shown in Fig. 1. The band at 3,440 was attributed to the O–H (hydroxyl or carboxyl) stretching vibration and C–OH (hydroxyl, ester, or ether) bending vibrations [40]. The two peaks at 1,710 and 1,640 cm⁻¹ were correspond to C=O stretching of the aromatic carboxylic moiety (C₆H₅–C=O) [43]. Obviously, all materials were rich in OFGs such as carboxyl and hydroxyls, moreover, and it was much more significant that the intensity of the adsorption bands at 1,710 and 1,640 cm⁻¹ increased gradually along with the rise of the heat treatment temperature. The results provided more direct evidence that heat treatment had a great influence on the content of carbonyl groups on HCSs. According to the results of Boehm titrations, the freshly carbonyl groups after heat treatment, especially at higher temperature, were mainly in the form of carboxyl groups.

The SEM images of pristine HCSs and HCSs-300 in Fig. 2 displayed that the carbon products appear to have perfect spherical shape, but seriously adhered. And the morphology of HCSs had no obvious changes after heat treatment.

3.2. The effect of solution pH

The pH of aqueous solution is an important variable for the Th(IV) adsorption on HCSs due to

Table 1

The influence of heating time and temperature on the weight-loss ratio, element, and carboxyl groups content

Sample	Weight-loss ratio ^a (%)	Element content (wt.%) ^b			Content of carboxyl groups (mmol/g)		
		C	H	O	1 h	3 h	5 h
Pristine HCSs	–	64.16	4.41	31.43		0.53	
HCSs-100	7.6	63.56	3.90	32.54	0.76	0.86	0.91
HCSs-150	10.1	62.08	3.97	33.95	1.27	1.35	1.44
HCSs-200	13.4	60.96	2.98	36.06	1.79	1.87	1.89
HCSs-250	22.7	59.20	2.76	38.04	2.11	2.52	2.70
HCSs-300	41.0	57.77	2.49	39.74	3.60	3.71	3.81

^aWeight-loss ratio was obtained by the ratio of the loss weight after heat treatment for 5 h to the weight of pristine HCSs.

^bThe samples tested element content was heat-treated for 5 h, and the oxygen content was calculated by subtracting the sum of carbon and hydrogen from 100.

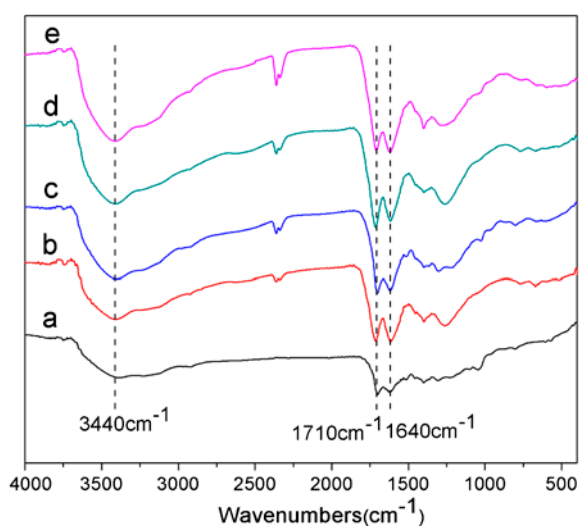


Fig. 1. FT-IR spectra of pristine HCSs (a), HCSs-100 (b), HCSs-200 (c), HCSs-250 (d), and HCSs-300 (e).

influencing the metal speciation and surface metal binding sites [12]. The effect of pH on the Th(IV) adsorption onto HCSs and HCSs-300 was carried out on the pH range 2.0–6.0 at 298.15 K, and the results are displayed in Fig. 3. The initial concentration of Th(IV) is 50 mg/L, due to the hydrolysis of thorium, so the concentration of Th(IV) under different pH was also displayed. The adsorption capacity of Th(IV), as well as the removal ratio was strongly affected by the solution pH. The sorption amount of HCSs and HCSs-300 increased from pH 2.0 to 3.5 and reached the maximum adsorption capacity of 12.62 and 42.67 mg/g at pH 3.5 and then declined. Simultaneously, the removal of Th(IV) due to adsorption and precipitation increased sharply from pH 3.0 to 6.0 and reached

about 90% at pH 6.0. Therefore, the efficiency of Th(IV) onto HCSs and HCSs-300 could be controlled by the initial pH of the solid/liquid reaction. The reaction for low adsorption capacity in high acidity was the competition between the excess of H⁺ ions and positively charged cations species present in the medium [12]. Th(IV) has a very complex chemistry in terms of hydrolysis, such as [Th(OH)]³⁺, [Th(OH)₂]²⁺, [Th(OH)₃]⁺, and Th(OH)₄ [3], then the increasing of pH led to a decrease in positive surface charge, which results in lower electrostatic pull of the charged Th(IV) hydrolysis products and the negative charged group of HCSs. Therefore, we speculated that the obtained removal ratio after pH 3.5 was due to the sorption of Th(IV) and the precipitation of Th(OH)₄. The solution pH at 3.5 was selected as the optimal value for adsorption of Th(IV) on HCSs and used for the following experiments.

3.3. The effect of heat treatment temperature

The previous research indicated that the pH of solution is one of the most crucial parameters for the Th(IV) adsorption, which can affect the surface charge, the metal speciation and surface metal binding sites. The optimal adsorption pH value of HCSs was 3.5. The effect of heat treatment temperature on the Th(IV) adsorption onto HCSs was carried out using 50 μg/mL initial thorium concentration at 298.15 K, and the results are displayed in Fig. 4. The sorption capacity of pristine HCSs was 11.56 mg/g and greatly increased to 33.88 mg/g when heat-treated at 250°C and then grew more slowly subsequently, which could be attributed to the newly generated carbonyl groups on the surface of carbon spheres acting as the Th(IV) adsorption activity sites.

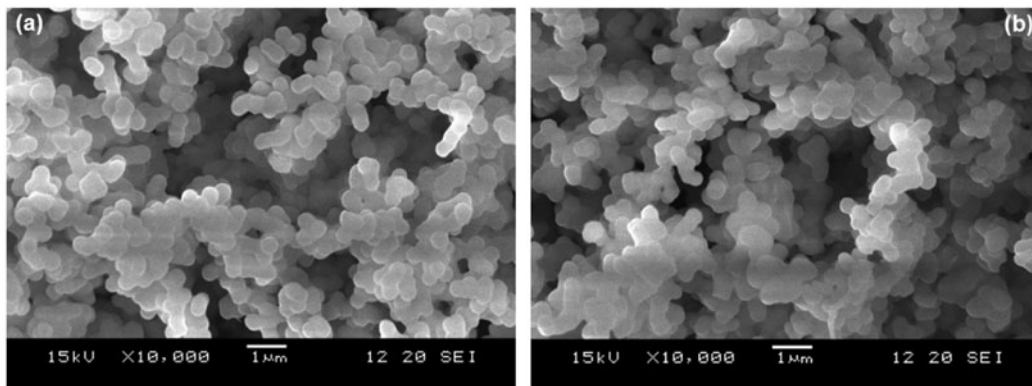


Fig. 2. SEM images of HCSs (a) and HCSs-300 (b).

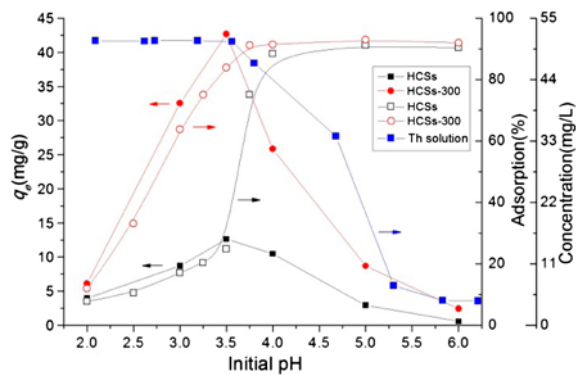


Fig. 3. The effect of initial solution pH on Th(IV) adsorption onto HCSs and HCSs-300 ($C_0 = 50 \text{ mg/L}$, $t = 120 \text{ min}$, $V = 50 \text{ mL}$, $T = 298.15 \text{ K}$, and $W = 50 \text{ mg}$).

3.4. The effect of contact time

The effect of contact time on adsorption of Th(IV) on HCSs and HCSs-300 was investigated to determine the equilibrium point. The variation of adsorption amount with vibrating time was studied using $50 \mu\text{g/mL}$ initial Th(IV) concentration at pH 3.5 and 298.15 K. As shown in Fig. 5, the uptake of Th(IV) onto HCSs and HCSs-300 increased sharply at the beginning and then gradually reached equilibrium after 80 min. Therefore, shaking time of 80 min was found to be appropriate for maximum sorption of Th(IV) on HCSs and HCSs-300 and was used in all subsequent experiments.

3.5. Adsorption kinetics

In order to explain the controlling mechanism of adsorption processes such as mass transfer and chemical reaction, pseudo-first-order and pseudo-second-order kinetic equations were applied to describe the

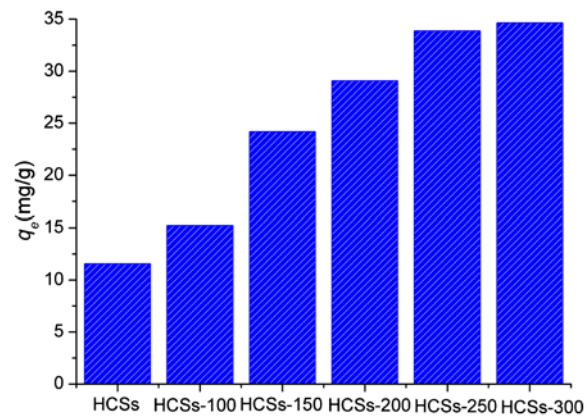


Fig. 4. The influence of heating temperature on the Th(IV) adsorption capacity of HCSs ($C_0 = 50 \text{ mg/L}$, $t = 120 \text{ min}$, $V = 50 \text{ mL}$, $T = 298.15 \text{ K}$, pH = 3.5, and $W = 50 \text{ mg}$).

kinetic characteristic of Th(IV) onto HCSs. The pseudo-first-order kinetic model is usually given as Eq. (3) [44].

$$\ln(q_e - q_t) = \ln q_e - k_1 t \quad (3)$$

where k_1 (min^{-1}) is the rate constant of first-order adsorption, q_e and q_t are the amounts of Th(IV) adsorbed (mg/g) at equilibrium and time “ t ”, respectively. Using Eq. (3), linear plot of $\ln(q_e - q_t)$ vs. t was plotted (Fig. 6). The k_1 , $q_{e, \text{cal}}$, and correlation coefficient (R^2) were calculated from the plot and presented in Table 2.

The pseudo-second-order kinetic model is always given as Eq. (4) [45].

$$\frac{t}{q_t} = \frac{1}{k_2 q_e^2} + \frac{t}{q_e} \quad (4)$$

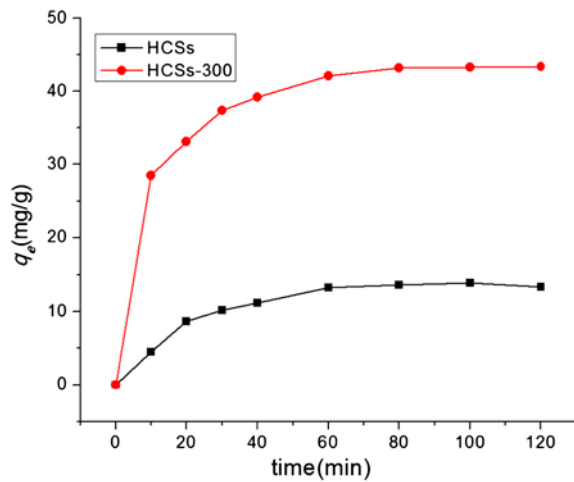


Fig. 5. The effect of contact time on Th(IV) adsorption onto HCSs and HCSs-300 ($C_0 = 50$ mg/L, $V = 50$ mL, $\text{pH} = 3.5$, $T = 298.15$ K, $\text{pH} = 3.5$, and $W = 50$ mg).

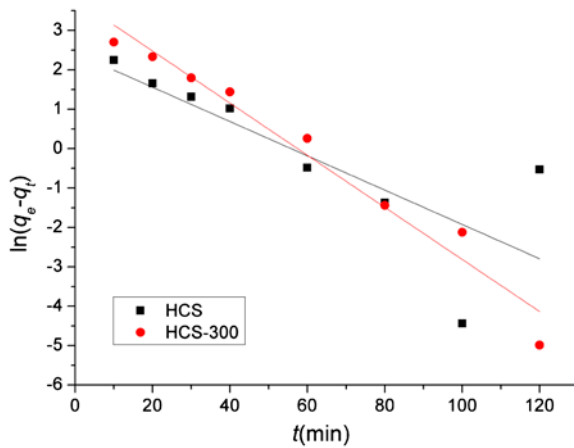


Fig. 6. The pseudo-first-order adsorption kinetics.

where k_2 (min^{-1}) is the rate constant of second-order adsorption. Using Eq. (4), linear plot of t/q_t vs. t was plotted (Fig. 7). The k_2 , $q_{e,\text{cal}}$, and correlation coefficient (R^2) were calculated from the plot and presented in Table 2.

As shown in Table 2, the square of correlation coefficients (R^2) of pseudo-second-order equation was better than the value of the pseudo-first-order equation. Moreover, the values of the amounts of Th(IV) adsorbed on HCSs and HCSs-300 at equilibrium, $q_{e,\text{cal}}$ (16.39 and 47.62 mg/g) were very close to the experimental values, $q_{e,\text{exp}}$ (13.67 and 43.30 mg/g). Therefore, the adsorption process was more in favor of the pseudo-second-order equation, which indicated that adsorption involved chemical reaction in adsorption in addition to physical adsorption [46].

3.6. Effect of initial Th(IV) concentration

The initial concentration provides an important driving force to overcome all mass transfer resistance of thorium between the aqueous and solid phases [47]. The effect of initial Th(IV) concentration on sorption was studied at 288.15–318.15 K and revealed in Fig. 8 and Fig. 9. The adsorptive capacity increased with the increase in the initial Th(IV) concentration until equilibrium was reached. The maximum adsorption capacities of HCSs and HCSs-300 were found to be 15.13 and 57.50 mg g^{-1} , respectively, at 308.15 K.

3.7. Adsorption isotherm

The equilibrium adsorption isotherms are one of the essential data to understand the mechanism of the adsorption systems. Langmuir and Freundlich equations are the most frequently used for describing sorption isotherms. The Langmuir model is based on assumptions of adsorption homogeneity such as equally available adsorption sites, monolayer surface coverage, and no interaction between adsorbed species. The Langmuir equation can be described by the linearized Eq. (5) [48].

$$\frac{C_e}{q_e} = \frac{1}{q_m K_L} + \frac{C_e}{q_m} \quad (5)$$

where C_e is the equilibrium concentration (mg/L), q_e is the amount of solute sorbed per unit weight of

Table 2
Adsorption kinetics of Th(IV) adsorption onto HCSs

Adsorbents	$q_{e,\text{exp}}$ (mg/g)	Pseudo-first-order kinetics			Pseudo-second-order kinetics		
		$q_{e,\text{cal}}$ (mg g^{-1})	k_1 (min^{-1})	R^2	$q_{e,\text{cal}}$ (mg/g)	k_2 (min^{-1})	R^2
HCSs	13.67	11.35	4.4×10^{-2}	0.575	16.39	3.2×10^{-3}	0.983
HCSs-300	43.30	44.68	6.6×10^{-2}	0.960	47.62	3.0×10^{-3}	0.999

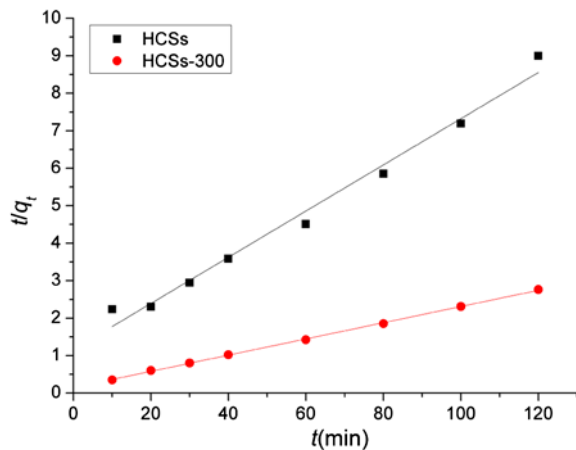


Fig. 7. Pseudo-second-order adsorption kinetics.

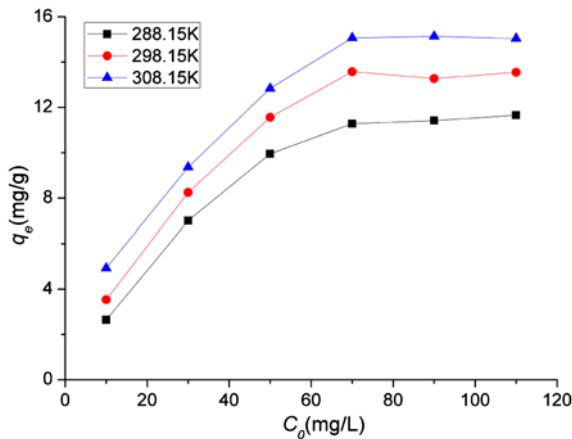


Fig. 8. The effect of initial concentration on Th(IV) adsorption onto HCSs ($V = 50$ mL, $pH = 3.5$, $t = 80$ min, $T = 298.15$ K, and $W = 50$ mg).

sorbent (mg/g), q_m is the Langmuir constant, which represents the saturated monolayer sorption capacity (mg/g). K_L is a constant related to the energy of adsorption.

The Freundlich model can be applied to nonideal sorption on heterogeneous surfaces as well as multi-layer sorption [49]. The empirical Freundlich equation can also be transformed into linearized Eq. (6).

$$\ln q_e = \ln K_F + \frac{1}{n} \ln C_e \quad (6)$$

where C_e is the equilibrium concentration (mg/L), q_e is the amount of solute sorbed per unit weight of sorbent (mg/g), K_F is the Freundlich constant related to

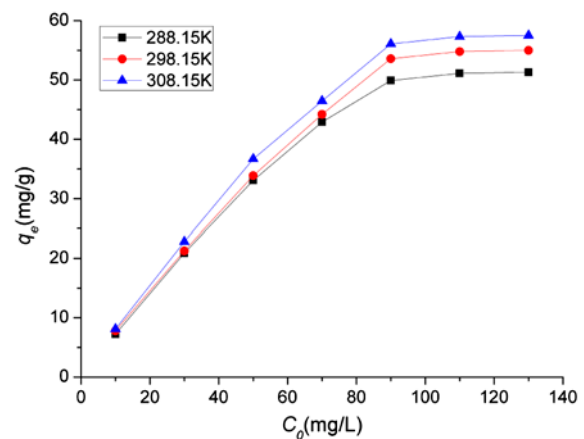


Fig. 9. The effect of initial concentration on Th(IV) adsorption onto HCSs-300 ($V = 50$ mL, $pH = 3.5$, $t = 80$ min, $T = 298.15$ K, and $W = 50$ mg).

the adsorption capacity, and n is relevant to the adsorption intensity.

The linearized form of Langmuir and Freundlich adsorption isotherms obtained from Figs. 8 and 9 is presented in Figs. 10–13, respectively. And the adsorption constants evaluated from the isotherms with the correlation coefficients (R^2) are given in Table 3. The value of R^2 showed that Langmuir isotherm model fitted better with the experimental data than Freundlich isotherm model. Moreover, the saturated monolayer sorption capacities (q_m) of HCSs and HCSs-300 were 15.79, 17.14, 17.76, and 65.06, 69.44, 69.93 mg/g, namely with the increase in temperature, the saturated monolayer sorption capacity added, which indicated that the sorption of Th(IV) onto HCSs and HCSs-300 was endothermic.

3.8. Adsorption thermodynamics

Thermodynamic parameters such as enthalpy (ΔH°), entropy (ΔS°), and Gibbs free energy (ΔG°) are useful in defining whether the sorption reaction is endothermic or exothermic, and spontaneity of the adsorption process [50]. The thermodynamic data are calculated using the following Eqs. (7) and (8).

$$\ln k_d = \frac{\Delta S^\circ}{R} - \frac{\Delta H^\circ}{RT} \quad (7)$$

$$\Delta G^\circ = \Delta H^\circ - T\Delta S^\circ \quad (8)$$

where k_d is the distribution coefficient (mL/g), ΔS° is the change of entropy (J/mol·K), ΔH° is the change of enthalpy (kJ/mol), T is the absolute temperature in

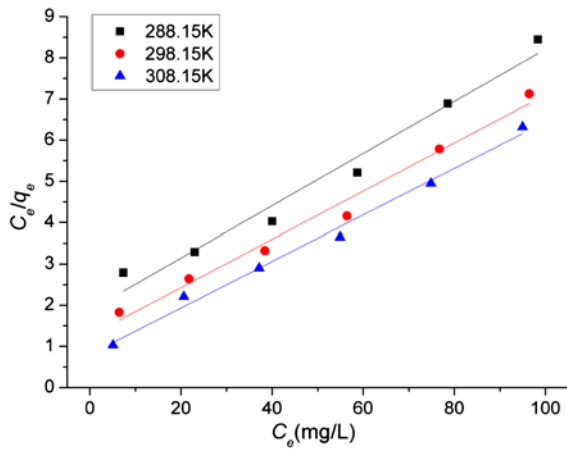


Fig. 10. The Langmuir adsorption isotherm models of Th (IV) adsorption onto HCSs.

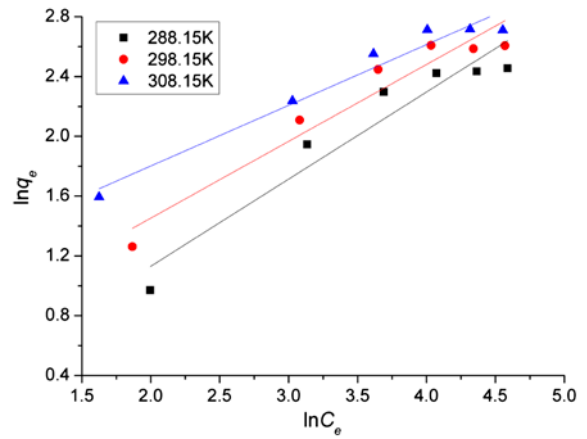


Fig. 12. The Freundlich adsorption isotherm models of Th (IV) adsorption onto HCSs.

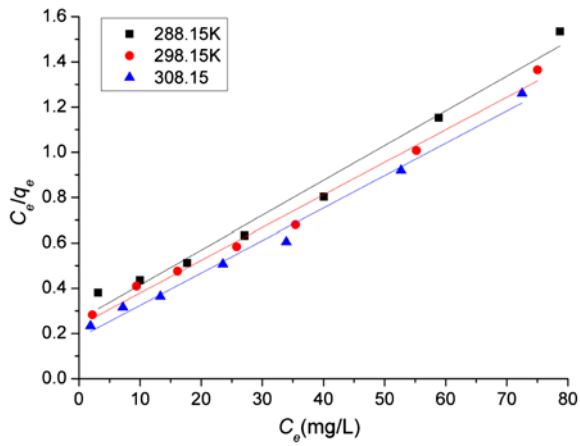


Fig. 11. The Langmuir adsorption isotherm models of Th (IV) adsorption onto HCSs-300.

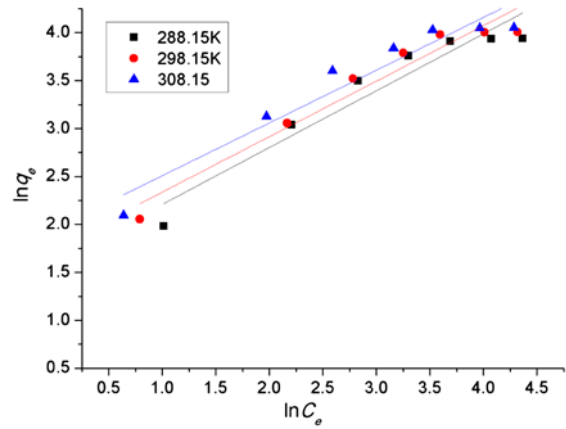


Fig. 13. The Freundlich adsorption isotherm models of Th (IV) adsorption onto HCSs-300.

Table 3
Isotherm constants and correlation coefficient for Th(IV) adsorption onto HCSs

Adsorbents	T (K)	Langmuir isotherm			Freundlich isotherm		
		K_L	q_m (mg/g)	R^2	n	K_F	R^2
HCSs	288.15	0.0337	15.79	0.968	1.72	0.97	0.905
	298.15	0.0463	17.14	0.981	1.95	1.53	0.918
	308.15	0.0698	17.76	0.989	2.46	2.69	0.951
HCSs-300	288.15	0.0589	65.06	0.980	1.68	5.02	0.908
	298.15	0.0612	69.44	0.987	1.72	5.80	0.937
	308.15	0.0787	69.93	0.989	1.82	7.08	0.917

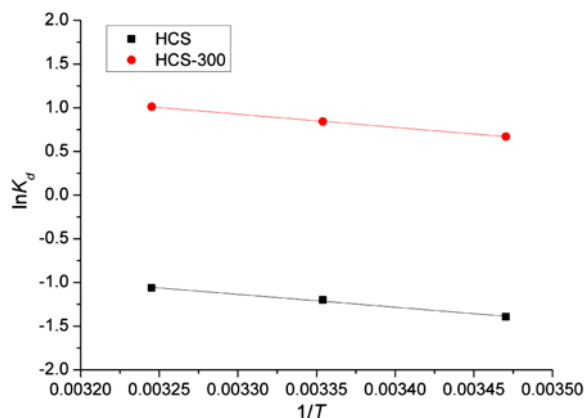


Fig. 14. The adsorption thermodynamics of Th(IV) on HCSs.

Kelvin (K), and R is the gas constant (8.314 J/mol·K). ΔH° and ΔS° can be calculated from the slope and intercept of the straight line (Fig. 14). The change of Gibbs free energy values is calculated from Eq. (8).

The values of thermodynamic parameters for the sorption of Th(IV) at different temperature are given in Table 4. The positive value of enthalpy change ΔH indicated that the sorption process was endothermic. The negative value of ΔG° at different temperatures confirmed the feasibility and spontaneous nature of adsorption process. Further, the increase in the value ΔG° with the decreasing temperature indicated that higher temperature favored the sorption process. The positive value of ΔS° reflected the affinity of the HCSs and HCSs-300 for Th(IV) and confirmed the increased randomness at the solid–solution interface during adsorption.

3.9. The effect of ionic strength

The effect of ionic strength on the adsorption capability of HCSs-300 was investigated. The ionic strength of Th(IV) solutions was adjusted by varying the concentration of KNO_3 in the range of 0.01–0.3 mol/L. As shown in Fig. 15, an increase in the ionic strength

from 0.01 to 0.1 mol/L had a rapid decrease in the amount of Th(IV) ions adsorbed and had little effect from 0.1 to 0.3 mol/L. The sorption capacity of Th(IV) was 30.27 mg/g at the K^+ concentration of 0.01 mol/L and declined to 17.19 mg/g at 0.1 mol/L. This phenomenon could be attributed to two reasons: (1) The presence of KNO_3 in the solution which screened the electrostatic interaction between the charges on HCSs-300 surface and the Th(IV) ions in solution and also competed with the Th(IV) ions for surface adsorption sites. (2) Ionic strength of solution influenced the activity coefficient of Th(IV), which limited their transfer to sorbent's surface.

3.10. Selective adsorption

In order to further study the sorption selectivity of pristine HCSs and HCSs-300 for thorium, experiments were performed in a solutions containing eight foreign cations including thorium ion. The results in the Fig. 16 indicated that the HCSs-300 showed a better adsorption capacity toward Th(IV) than the co-existing ions.

Further, selectivity coefficient ($S_{\text{Th}^{4+}/\text{M}^{n+}}$) for thorium ions relative to competing ions was studied by the Eq. (9).

$$S_{\text{Th}^{4+}/\text{M}^{n+}} = \frac{K_d^{\text{Th}^{4+}}}{K_d^{\text{M}^{n+}}} \quad (9)$$

where $K_d^{\text{Th}^{4+}}$ and $K_d^{\text{M}^{n+}}$ are distribution coefficients of thorium ions and other ions, respectively.

The relative selectivity coefficient S_r is calculated according the Eq. (10).

$$S_r = \frac{S_{\text{HCSs-300}}}{S_{\text{HCSs}}} \quad (10)$$

The results of K_d , $S_{\text{Th}^{4+}/\text{M}^{n+}}$ and S_r are listed in the Table 5. As it could be seen that the values of K_d , $S_{\text{Th}^{4+}/\text{M}^{n+}}$ and S_r of HCSs-300 were much greater than HCSs, therefore the selective properties of HCSs toward Th(IV) were improved by heat treatment.

Table 4
The thermodynamic parameters of Th(IV) adsorption onto HCSs

Adsorbents	ΔH° (kJ/mol)	ΔS° (J/mol K)	ΔG° (kJ/mol)		
			288.15 K	298.15 K	308.15 K
HCSs	12.20	30.82	−8.87	−9.18	−9.48
HCSs-300	12.61	49.31	−14.20	−14.69	−15.18

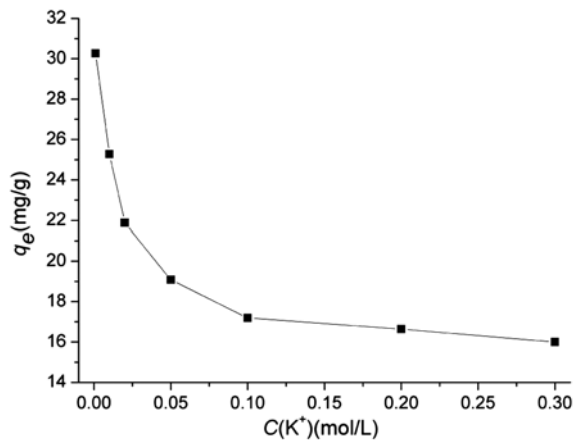


Fig. 15. The effect of ionic strength on Th(IV) adsorption onto HCSs-300 ($C_0 = 50$ mg/L, pH = 3.5, $t = 80$ min, $V = 50$ mL, $T = 298.15$ K, and $W = 50$ mg).

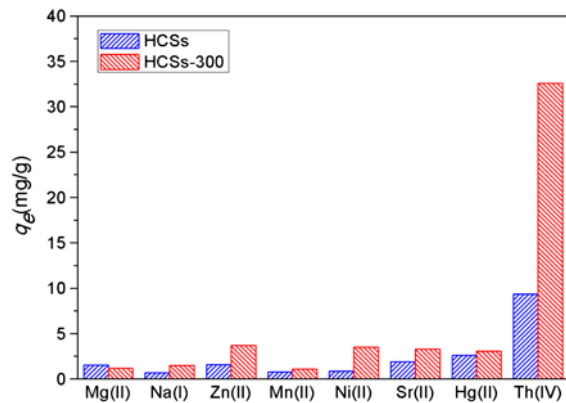


Fig. 16. Selective sorption capacity of coexistent ions ($C_0 = 10$ mg/L, pH = 3.5, $t = 80$ min, $V = 150$ mL, $T = 298.15$ K, and $W = 40$ mg).

3.11. Desorption and regeneration

Repeated availability is an important factor for an advanced adsorbent. Such adsorbent not only possesses higher adsorption capability, but also shows better desorption property, which will significantly reduce overall cost for adsorbent. Desorption tests of HCSs-300 were tried with HCl solutions in the concentration range from 0.1 to 2.0 mol/L. As shown in Fig. 17, higher acidity promoted the desorption progress. So, the reusability experiments were conducted adopting 1.0 mol/L HCl as desorbing agent and the results are shown in Table 6. After five consecutive sorption/desorption cycles, the sorption capability decreased from 42.67 mg/g in the first cycle to 35.86 mg/g in the fifth cycle, while the recovery of Th(IV) ions decreased from 98.56 to 90.12%. The results indicated HCSs-300 could be efficiently regenerated by 1.0 mol/L HCl and reused with only slight impact on its Th(IV) sorption capability after five cycles.

3.12. Test with artificial seawater

In order to demonstrate the adsorption potential of HCSs-300, experiments were performed in simulated seawater. Simulated seawater containing 25.0 mg/L Th(IV) having the composition NaCl (41.5 g/L), Na_2SO_4 (6.9 g/L), KCl (1.1 g/L), $NaHCO_3$ (0.34 g/L), KBr (0.16 g/L), H_3BO_3 (0.16 g/L), NaF (5.00 mg/L), $MgCl_2 \cdot 6H_2O$ (18.79 g/L), $CaCl_2 \cdot 2H_2O$ (2.63 g/L), and $SrCl_2 \cdot 6H_2O$ (0.04 g/L) was used [51]. The effect of adsorbent dose on the removal of Th(IV) from seawater was investigated (Fig. 18). It was observed that the percentage removal of thorium increased with increase in the mass of HCSs-300 and almost complete removal ($\approx 100\%$) of Th(IV) from the wastewater containing 25.0 mg/L was achieved with 1.5 g HCSs-300 in 1.0 L.

Table 5
Selective adsorption properties of pristine HCSs and HCSs-300

Elements	K_d (mL/g)		S		S_r
	Pristine HCSs	HCSs-300	Pristine HCSs	HCSs-300	
Th(IV)	687.87	9005.10	–	–	–
Mg(II)	159.84	117.98	7.78	210.85	27.11
Na(I)	64.87	157.84	19.17	157.60	8.22
Zn(II)	164.24	407.28	7.57	61.08	8.07
Mn(II)	78.81	110.75	15.78	224.61	14.24
Ni(II)	92.89	389.42	13.39	63.88	4.77
Sr(II)	195.33	360.10	6.37	69.08	10.85
Hg(II)	280.04	333.44	4.44	74.60	16.80

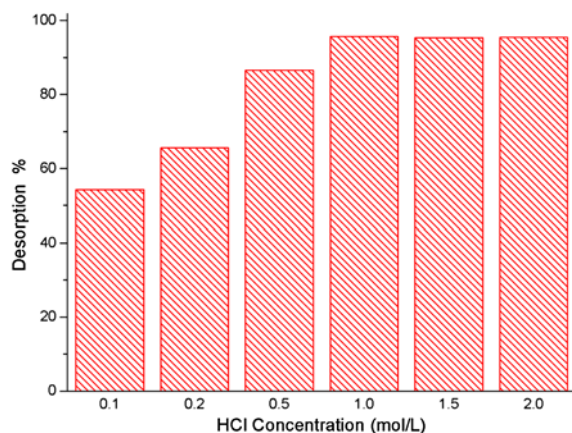


Fig. 17. Effect of HCl concentration on Th(IV) desorption.

Table 6

Five cycles of uranium adsorption–desorption with 0.1 mol/L HCl as desorbing agent

Cycle	Adsorption		Desorption (%)
	Capacity (mg/g)	Removal (%)	
1	42.67	0.85	98.56
2	40.13	0.80	97.48
3	39.56	0.79	95.26
4	36.73	0.73	93.13
5	35.86	0.72	90.12

Table 7

Sorption capacity of Th(IV) on HCSs-300 with other adsorbents

Adsorbents	Sorption properties				References
	Temperature (K)	pH	Time (h)	Sorption capacity (mg/g)	
HCSs-300	298	3.5	1.33	69.44	This work
Perlite	303	4.5	0.5	4.40	[8]
Al-pillared rectorite	293 ± 2	1.88 ± 0.05	10	30.16	[11]
5-mercapto-1-methyltetrazole modified bentonite mineral	298 ± 1	2.0	24	29.61	[12]
Diatomite	303	2.5 ± 0.1	48	25.06	[16]
Alumina	298 ± 1	2.32 ± 0.05	6	17.40	[17]
Activated carbon	303	4.0	0.5	18.30	[19]
Oxidized multi-wall carbon nanotubes	293 ± 2	1.9 ± 0.02	1.0	12.76	[20]
Diglycolamide functionalized multi-walled carbon nanotubes	298	4.0	2.0	10.58	[21]
PAN/zeolite composite	303	4.0	0.75	40.83	[22]
PAMAM dendron-functionalized styrene divinyl benzene	298	5.0	2.0	36.20	[52]
Algae-yeast/silica gel biosorbent	298	4.0	2.0	26.95	[53]

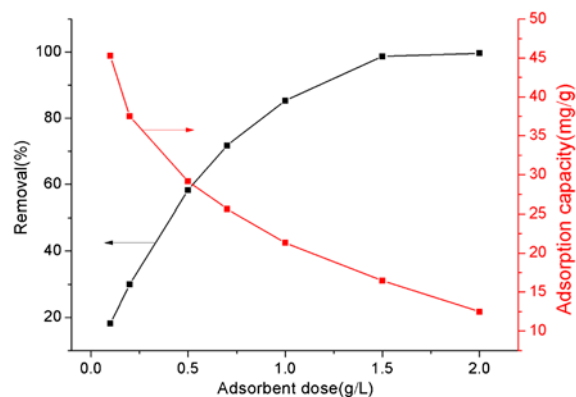


Fig. 18. Th(IV) ion removal from artificial seawater by HCSs-300.

3.13. Th(IV) sorption performance of HCSs-300 with other adsorbents

The Th(IV) sorption capacity of HCSs-300 was compared with other adsorbents, as shown in Table 7, the Th(IV) sorption capacity of HCSs-300 ($69.44 \text{ mg}\cdot\text{g}^{-1}$) at 298 K was even larger than that of Alumina ($17.40 \text{ mg}\cdot\text{g}^{-1}$) diglycolamide functionalized multi-walled carbon nanotubes ($10.58 \text{ mg}\cdot\text{g}^{-1}$) and PAMAM dendron-functionalized styrene divinyl benzene ($36.20 \text{ mg}\cdot\text{g}^{-1}$). Obviously, HCSs-300 was a perfect adsorbent toward Th(IV) with cheap price, large adsorption capacity, and ease of handling.

4. Conclusion

In this paper, hydrothermal carbon spheres (HCSs) with large number of carboxyl groups on the surface were prepared by simply heating at lower temperature in air, and the textural properties of carboxyl-rich hydrothermal carbon spheres were characterized using Boehm titrations, scanning electron microscopy, Fourier transform infrared spectrometer, and elemental analysis. The content of carboxyl groups on HCSs increased significantly from 0.53 to 3.81 mmol/g and the micro-morphology has not obviously changed after heat treatment at 300°C. The sorption performances were controlled by solution pH, heat treatment temperature, contact time, initial thorium concentration, temperature, and ionic strength. The Th(IV) sorption capacity of HCSs increased from 17.76 to 69.93 mg/g after heat treatment at 300°C for 5 h. The adsorption of Th(IV) from aqueous solution on HCSs and HCSs-300 was fitted to the Langmuir adsorption isotherms and pseudo-second-order kinetics models. And the thermodynamic parameters, such as ΔG° , ΔH° , and ΔS° , clearly indicated that the adsorption process was feasible, spontaneous, and endothermic in nature. Selective adsorption studies showed that the heat-treated HCSs could selectively remove Th(IV) in the solution containing a great deal of competing ions. Desorption and regeneration test indicated that HCSs-300 can be effectively regenerated and reused for Th(IV) sorption. The research results suggested that HCSs-300 may be a good candidate for application in selective separation of thorium from seawater and other Th-containing aqueous media.

Acknowledgments

This work is financially supported by the National Natural Science Foundation of China (Grant No. 21101024 and 21201033), Key Project of Chinese Ministry of Education (Grant No. 211086), Sci. & Tech. Project of Jiangxi Provincial department of education (No. GJJ13452), Open Project Foundation of the Key Laboratory of Radioactive Geology and Exploration Technology Fundamental Science for National Defense (East China Institute of Technology) (2010RGET08, RGET1218), Open Project Foundation of the Engineering Research Center of Nano-Geomaterials of Ministry of Education (China University of Geosciences) (CUGNGM201205), and Open Project Foundation of the State Key Laboratory of Biogeology and Environmental Geology (China University of Geosciences) (BGEG201105).

References

- [1] H.S. Syed, Comparison studies adsorption of thorium and uranium on pure clay minerals and local Malaysian soil sediments, *J. Radioanal. Nucl. Chem.* 241 (1999) 11–14.
- [2] Y. Khazaei, H. Faghihian, M. Kamali, Removal of thorium from aqueous solutions by sodium clinoptilolite, *J. Radioanal. Nucl. Chem.* 289 (2011) 529–536.
- [3] T.S. Anirudhan, S. Rijith, A.R. Tharun, Adsorptive removal of thorium(IV) from aqueous solutions using poly(methacrylic acid)-grafted chitosan/bentonite composite matrix: Process design and equilibrium studies, *Colloids Surf., A* 368 (2010) 13–22.
- [4] B. Venugopal, T.P. Luckey, Toxicology of non-radioactive heavy metals and their salts, *Environ. Qual. Saf. Suppl.* 1 (1975) 4–73.
- [5] T. Sato, Liquid-liquid extraction of thorium(IV) from hydrochloric acid solutions by dihexyl sulphoxide, *Solvent. Extr. Res. Dev. Jpn.* 15 (2008) 61–69.
- [6] M.A. Bayyari, M.K. Nazal, F.A. Khalili, The effect of ionic strength on the extraction of Thorium(IV) from nitrate solution by didodecylphosphoric acid (HDDPA), *J. Saudi Chem. Soc.* 14 (2010) 311–315.
- [7] F.H. El-Sweify, M.K.K. Shehata, E.A.A. El-Shazly, Ion exchange studies of Arsenazo-III and thorium(IV) from aqueous solutions of Arsenazo-III with AG-2×8, Dowex-50 W×8 and Chelex-100, *J. Radioanal. Nucl. Chem. Art.* 198 (1995) 77–87.
- [8] Z. Talip, M. Eral, Ü. Hiçsönmez, Adsorption of thorium from aqueous solutions by perlite, *J. Environ. Radioact.* 100 (2009) 139–143.
- [9] Z. Hongxia, D. Zheng, T. Zuyi, Sorption of thorium (IV) ions on gibbsite: Effects of contact time, pH, ionic strength, concentration, phosphate and fulvic acid, *Colloids Surf., A* 278 (2006) 46–52.
- [10] D.L. Zhao, S.J. Feng, C.L. Chen, S.H. Chen, D. Xu, Adsorption of thorium(IV) on MX-80 bentonite: Effect of pH, ionic strength and temperature, *Appl. Clay Sci.* 41 (2008) 17–23.
- [11] S.M. Yu, C.L. Chen, P.P. Chang, T.T. Wang, S.S. Lu, Adsorption of Th(IV) onto Al-pillared rectorite: Effect of pH, ionic strength, temperature, soil humic acid and fulvic acid, *Appl. Clay Sci.* 38 (2008) 219–226.
- [12] D. Baybaş, U. Ulusoy, The use of polyacrylamide-aluminosilicate composites for thorium adsorption, *Appl. Clay Sci.* 51 (2011) 138–146.
- [13] D.L. Guerra, R.R. Viana, C. Airoidi, Adsorption of thorium cation on modified clays MTTZ derivative, *J. Hazard. Mater.* 168 (2009) 1504–1511.
- [14] D.L. Guerra, R.R. Viana, C. Airoidi, Adsorption of thorium(IV) on chemically modified Amazon clays, *J. Braz. Chem. Soc.* 20 (2009) 1164–1174.
- [15] D.L. Guerra, R.R. Viana, L.P. da Costa, C. Airoidi, Retraction notice to Sodium alginate films modified by raw and functionalized attapulgite for use of thorium(IV) adsorption: A thermodynamic approach, *J. Phys. Chem. Solids* 73 (2012) 142.
- [16] G. Sheng, J. Hu, X. Wang, Sorption properties of Th (IV) on the raw diatomite—Effects of contact time, pH, ionic strength and temperature, *Appl. Radiat. Isot.* 66 (2008) 1313–1320.
- [17] Z.J. Guo, X.M. Yu, F.H. Guo, Z.Y. Tao, Th(IV) adsorption on alumina: Effects of contact time, pH, ionic

- strength and phosphate, *J. Colloid Interface Sci.* 288 (2005) 14–20.
- [18] T. Tsuruta, Cell-associated adsorption of thorium or uranium from aqueous system using various microorganisms, *Water Air Soil Pollut.* 159 (2004) 35–47.
- [19] C. Kütahyalı, M. Eral, Sorption studies of uranium and thorium on activated carbon prepared from olive stones: kinetic and thermodynamic aspects, *J. Nucl. Mater.* 396 (2010) 251–256.
- [20] C. Chen, X. Li, D. Zhao, X. Tan, X. Wang, Adsorption kinetic, thermodynamic and desorption studies of Th (IV) on oxidized multi-wall carbon nanotubes, *Colloids Surf., A* 302 (2007) 449–454.
- [21] A.K.S. Deb, B.N. Mohanty, P. Ilaiyaraja, K. Sivasubramanian, B. Venkatraman, Adsorptive removal of thorium from aqueous solution using diglycolamide functionalized multi-walled carbon nanotubes, *J. Radioanal. Nucl. Chem.* 295 (2013) 1161–1169.
- [22] A.K. Kaygun, S. Akyil, Study of the behaviour of thorium adsorption on PAN/zeolite composite adsorbent, *J. Hazard. Mater.* 147 (2007) 357–362.
- [23] M.G. Salinas-Pedroza, M.T. Olguín, Thorium removal from aqueous solutions of Mexican erionite and X zeolite, *J. Radioanal. Nucl. Chem.* 260 (2004) 115–118.
- [24] T.S. Anirudhan, S.R. Rejeena, Thorium (IV) removal and recovery from aqueous solutions using tannin-modified poly (glycidylmethacrylate)-grafted zirconium oxide densified cellulose, *Ind. Eng. Chem. Res.* 50 (2011) 13288–13298.
- [25] Y. Zhao, C. Liu, M. Feng, Z. Chen, S. Li, G. Tian, L. Wang, J. Huang, S. Li, Solid phase extraction of uranium(VI) onto benzoylthiourea-anchored activated carbon, *J. Hazard. Mater.* 176 (2010) 119–124.
- [26] S.J. Coleman, P.R. Coronado, R.S. Maxwell, J.G. Reynolds, Granulated activated carbon modified with hydrophobic silica aerogel-potential composite materials for the removal of uranium from aqueous solutions, *Environ. Sci. Technol.* 37 (2003) 2286–2290.
- [27] D. Shao, Z. Jiang, X. Wang, J. Li, Y. Meng, Plasma induced grafting carboxymethyl cellulose on multi-walled carbon nanotubes for the removal of UO_2^{2+} from aqueous solution, *J. Phys. Chem. B* 113 (2009) 860–864.
- [28] A. Schierz, H. Zänker, Aqueous suspensions of carbon nanotubes: surface oxidation, colloidal stability and uranium sorption, *Environ. Pollut.* 157 (2009) 1088–1094.
- [29] Y. Xu, J.W. Zondlo, H.O. Finklea, A. Brennstainer, Electrosorption of uranium on carbon fibers as a means of environmental remediation, *Fuel Process. Technol.* 68 (2000) 189–208.
- [30] Y.Q. Wang, Z.B. Zhang, Y.H. Liu, X.H. Cao, Y.T. Liu, Q. Li, Adsorption of U(VI) from aqueous solution by the carboxyl-mesoporous carbon, *Chem. Eng. J.* 198–199 (2012) 246–253.
- [31] Q. Song, L. Ma, J. Liu, C. Bai, J. Geng, H. Wang, B. Li, L. Wang, S. Li, Preparation and adsorption performance of 5-azacytosine-functionalized hydrothermal carbon for selective solid-phase extraction of uranium, *J. Colloid. Interf. Sci.* 386 (2012) 291–299. doi:10.1016/j.jcis.2012.07.070.
- [32] Q. Wang, H. Li, L. Chen, X. Huang, Monodispersed hard carbon spherules with uniform nanopores, *Carbon* 39 (2001) 2211–2214.
- [33] Y. Mi, W. Hu, Y. Dan, Y. Liu, Synthesis of carbon micro-spheres by a glucose hydrothermal method, *Mater. Lett.* 62 (2008) 1194–1196.
- [34] M. Zheng, J. Cao, X. Chang, J. Wang, J. Liu, X. Ma, Preparation of oxide hollow spheres by colloidal carbon spheres, *Mater. Lett.* 60 (2006) 2991–2993.
- [35] Z.H. Zhuang, Z.G. Yang, Preparation and characterization of colloidal carbon sphere/rigid polyurethane foam composites, *J. Appl. Polym. Sci.* 114 (2009) 3863–3869.
- [36] C. Yao, Y. Shin, L.Q. Wang, C.F. Windisch, W.D. Samuels, B.W. Arey, C. Wang, W.M. Risen, G.J. Exarhos, Hydrothermal dehydration of aqueous fructose solutions in a closed system, *J. Phys. Chem. C* 111 (2007) 15141–15145.
- [37] M. Sevilla, A.B. Fuertes, The production of carbon materials by hydrothermal carbonization of cellulose, *Carbon* 47 (2009) 2281–2289.
- [38] Y. Shen, Y. Lin, M. Li, C.W. Nan, High dielectric performance of polymer composite films induced by a percolating interparticle barrier layer, *Adv. Mater.* 19 (2007) 1418–1422.
- [39] M.M. Titirici, M. Antonietti, Chemistry and materials options of sustainable carbon materials made by hydrothermal carbonization, *Chem. Soc. Rev.* 39 (2010) 103–116.
- [40] M. Sevilla, A.B. Fuertes, Chemical and structural properties of carbonaceous products obtained by hydrothermal carbonization of saccharides, *Chem. Eur. J.* 15 (2009) 4195–4203.
- [41] Z. Zhang, W. Nie, Q. Li, G. Xiong, X. Cao, Y. Liu, Removal of uranium(VI) from aqueous solutions by carboxyl-rich hydrothermal carbon spheres through low-temperature heat treatment in air, *J. Radioanal. Nucl. Chem.* 298 (2013) 361–368.
- [42] H.P. Boehm, Some aspects of the surface chemistry of carbon blacks and other carbons, *Carbon* 32 (1994) 759–769.
- [43] X. Sun, Y. Li, Ag@ C core/shell structured nanoparticles: controlled synthesis, characterization, and assembly, *Langmuir* 21 (2005) 6019–6024.
- [44] A. Ghaemi, M. Torab-Mostaedi, M. Ghannadi-Maraagheh, Characterizations of strontium(II) and barium (II) adsorption from aqueous solutions using dolomite powder, *J. Hazard. Mater.* 190 (2011) 916–921.
- [45] T. Psareva, O. Zakutevskyy, N. Chubar, V. Strelko, T. Shaposhnikova, J. Carvalho, M. Correia, Uranium sorption on cork biomass, *Colloids Surf., A* 252 (2005) 231–236.
- [46] T.S. Anirudhan, S. Rijith, A.R. Tharun, Adsorptive removal of thorium(IV) from aqueous solutions using poly(methacrylic acid)-grafted chitosan/bentonite composite matrix: Process design and equilibrium studies, *Colloids Surf., A* 368 (2010) 13–22.
- [47] S. Aytas, M. Yurtlu, R. Donat, Adsorption characteristic of U(VI) ion onto thermally activated bentonite, *J. Hazard. Mater.* 172 (2009) 667–674.
- [48] O. Hazer, Ş. Kartal, Use of amidoximated hydrogel for removal and recovery of U(VI) ion from water samples, *Talanta* 82 (2010) 1974–1979.
- [49] H. Parab, S. Joshi, N. Shenoy, R. Verma, A. Lali, M. Sudersanan, Uranium removal from aqueous solution by coir pith: equilibrium and kinetic studies, *Biore-sour. Technol.* 96 (2005) 1241–1248.

- [50] T.S. Anirudhan, L. Divya, P.S. Suchithra, Kinetic and equilibrium characterization of uranium(VI) adsorption onto carboxylate-functionalized poly(hydroxyethylmethacrylate)-grafted lignocellulosics, *J. Environ. Manage.* 90 (2009) 549–560.
- [51] T.R. Parsons, Y. Maita, C.M. Lalti, *A Manual of Chemical and Biological Methods for Seawater Analysis*. Pergamon Press Inc, Elmsford, New York, NY, 1984, pp.395.
- [52] P. Ilaiyaraja, A.K.S. Deb, K. Sivasubramanian, Removal of thorium from aqueous solution by adsorption using PAMAM dendron-functionalized styrene divinyl benzene, *J. Radioanal Nucl. Chem.* 297 (2013) 59–69.
- [53] C. Gok, Removal of Th(IV) ions from aqueous solution using bi-functionalized algae-yeast biosorbent, *J. Radioanal. Nucl. Chem.* 287 (2011) 533–541.